Supplementary Information

A single-ion conducting covalent organic frameworks for aqueous rechargeable Zn-ion batteries

Sodam Park,[a] Imanuel Kristanto,[b] Gwan Yeong Jung,[b] David B. Ahn,[a]
Kihun Jeong*[a], Sang Kyu Kwak*[a] and Sang-Young Lee*[c]

[a]Department of Energy Engineering and [b]Department of Chemical Engineering, School of Energy and Chemical Engineering, Ulsan National Institute of Science and Technology (UNIST), Ulsan 44919, Korea

[c]Department of Chemical and Biomolecular Engineering, Yonsei University, 50 Yonsei-ro, Seodaemun-gu, Seoul 120-749, Republic of Korea

*E-mail: jkh1905@unist.ac.kr; skkwak@unist.ac.kr; sangyounglee87@gmail.com

Table of Contents

Experimental details

Materials

1,4-phenylenediamine-2-sulfonic acid (Pa-SO_3H), 1,4-dioxane, mesitylene, acetic acid, zinc acetate and polytetrafluoroethylene (PTFE, 60 wt% dispersion in H_2O) were purchased from Merck. The Zn metal foil (99.98%) was purchased from Alfa Aesar. 1,3,5-triformylphloroglucinol (Tp),[S1] the sulfonic acid COF (TpPa-SO_3H),[S2,S3] the non-sulfonated COF (TpPa)[S4] and α-MnO_2[S5] were synthesised as previously reported. All other chemicals were obtained from commercial sources and used as received unless otherwise noted.

Synthesis of TpPa-$SO_3Zn_{0.5}$

TpPa-SO_3H (605 mg) was suspended in a 1 M aqueous zinc acetate solution (40 mL) and stirred for 72 h at room temperature, during which the solution was exchanged at an interval of 24 h. The resultant powders were collected by filtration and washed with H_2O to ensure the removal of excess zinc acetate. After dried under vacuum at 120 ºC for overnight, the reddish powders of TpPa-$SO_3Zn_{0.5}$ were obtained (yield: 612 mg, 91%).

Structural and physicochemical characterisations

The elemental analysis was performed using a Leco TruSpec Micro CHN analyser. The Zn content was determined by inductively coupled plasma optical emission spectrometry (ICP-OES) using a Varian 700-ES. The Fourier transform infrared (FT-IR) spectrum was recorded using a Bruker ALPHA Laser class 1. The cross polarisation magic angle spinning ^{13}C nuclear magnetic resonance (CP-MAS ^{13}C NMR) experiment was performed using an Agilent VNMRS 600 MHz NMR spectrometer at a 20 kHz spinning rate. Chemical shifts were referenced to hexamethylbenzene at 17.3 ppm as an external standard. Morphological analyses were performed using a Hitachi S-4800 field-emission scanning electron microscope (FE-SEM) equipped with a JEOL JSM-6400 energy dispersive X-ray spectroscopy (EDS) detector and a Tecnai G2 F20 X-Twin transmission electron microscope (TEM) equipped with an Oxford INCA X-sight 7688 EDS detector. X-ray diffraction (XRD) patterns were recorded through a transmittance mode at the 6D UNIST-PAL beamline of the Pohang Accelerator Laboratory or using a Rigaku D/MAX2500. N_2 gas sorption isotherms were measured at 77 K with a Micromeritcs ASAP 2020 physisorption analyser. Brunauer–Emmett–Teller (BET) and non-

local density functional theory (NLDFT) methods were utilised to calculate the specific surface area and the pore size, respectively. The thermogravimetric analysis (TGA) was performed on a TA Instruments Q500 thermogravimetric analyser under a N_2 atmosphere at a heating rate of 10 ºC min^{-1}. Time-of-flight secondary ion mass spectroscopy (TOF-SIMS) mapping images were obtained using IONTOF TOF-SIMS 5. The X-ray photoelectron spectroscopy (XPS) analysis was conducted using a Thermo Fisher Scientific ESCALAB 250Xi.

Electrochemical characterisations

The self-standing TpPa-$SO_3Zn_{0.5}$ pellets were prepared by a cold-pressing method under *ca*. 40 MPa at room temperature. The flexible TpPa-$SO_3Zn_{0.5}$ membranes were prepared by mixing PTFE (5 wt%) with the TpPa-$SO_3Zn_{0.5}$ powders. The obtained pellets and membranes were hydrated before the electrochemical tests.

[Ionic conductivity]

Ionic conductivity was measured with Zn^{2+} blocking Ti|TpPa-$SO_3Zn_{0.5}$|Ti cells based on an electrochemical impedance spectroscopy (EIS) analysis in a frequency range from 10^{-2} to 10^6 Hz at an applied amplitude of 10 mV using a Bio-logic VSP classic potentiostat. The ionic conductivity (σ) was determined according to the following equation:

$$\sigma = \frac{l}{RA}$$

where l is the pellet (or membrane) thickness, R is the resistance and A is the area in contact with the electrodes. The control experiment without Zn^{2+} was conducted using a Ti|TpPa|Ti cell.

[Zn^{2+} transference number][S6]

The time-dependent current flowing through a Zn|TpPa-$SO_3Zn_{0.5}$|Zn cell and the impedance of the cell before and after direct current (DC) polarisation (20 mV) were measured. The Zn^{2+} transference number ($t_{Zn^{2+}}$) was determined according to the following equation:

$$t_{Zn^{2+}} = \frac{I_{ss}(\Delta V - I_0 R_0)}{I_0(\Delta V - I_{ss} R_{ss})}$$

where I_{ss} is the steady-state current, I_0 is the initial current, ΔV is the applied potential, R_0 and R_{ss} are the interfacial resistances before and after polarisation, respectively.

[Linear sweep voltammetry]

Linear sweep voltammetry (LSV) was conducted with a Zn|TpPa-$SO_3Zn_{0.5}$|Ti cell operated under a sweep rate of 0.2 mV s^{-1} in a voltage range from –0.2 to 3 V (vs. Zn/Zn^{2+}) at room temperature.

[Zn stripping/plating experiments]

The galvanostatic cyclability of a Zn|TpPa-$SO_3Zn_{0.5}$|Zn cell and a Zn|liquid electrolyte (LE)|Zn cell (LE = 2 M $ZnSO_4$ in H_2O) was examined at room temperature (current density = 0.1 mA cm^{-2}, capacity = 0.1 mAh cm^{-2}). The reversibility of Zn stripping/plating was investigated with the Zn||Ti configurations, in which Zn metal was electrochemically plated on the Ti working electrode and subsequently stripped out during a cycle (current density = 0.1 mA cm^{-2}, capacity = 0.1 mAh cm^{-2}). The Zn||Cu configurations were used for monitoring Zn electroplating behaviour (current density = 0.3 mA cm^{-2}, capacity = 3 mAh cm^{-2}).

[Zn//MnO_2 battery tests]

The electrode slurry composed of MnO_2, carbon black and polyvinylidene fluoride in a weight ratio of 7/2/1 was dispersed in N-methyl-2-pyrrolidone and casted onto a Ti foil current collector. The solvent was removed under vacuum at 60 ºC for overnight. The prepared MnO_2 cathode was immersed with an LE (2 M $ZnSO_4$ + 0.2 M $MnSO_4$ in H_2O) and assembled with TpPa-$SO_3Zn_{0.5}$ (or a glass fibre containing the LE) and a Zn metal anode. The resultant Zn||MnO_2 cells were tested under a current density of 0.6 A g^{-1} at room temperature.

Simulation details

Density functional theory (DFT) calculations

The structural model of TpPa-$SO_3Zn_{0.5}$ was constructed based on those reported for TpPa-SO_3X (X = H, Li),[S2,S3] in which Zn atoms were introduced upon consideration of the charge balance between the sulfonated framework and Zn^{2+}. The stable positions of Zn atoms were investigated by geometry optimisation. All DFT calculations were performed using $DMol^3$ program.[S7,S8] The generalised gradient approximation with Perdew–Burke–Ernzerhof functional (GGA-PBE)[S9] was used for the exchange-correlation energy. The double numerical polarisation basis set with spin-polarised calculations were used, while core-electron treatment was conducted with the DFT semi-core pseudopotential. The dispersion correction pertaining to van der Waals interactions was applied with semi-empirical Tkatchenko-Scheffler (TS)

scheme.[S10] The Brillouin zone was sampled by Monkhorst-Pack[S11] 1 × 1 × 2 *k*-point mesh for all systems. The self-consistent field (SCF) convergence for each electronic energy was set as 1.0×10^{-6} Ha. The convergence precision of geometry optimisation for energy, force and displacement were set to 1.0×10^{-5} Ha, 0.002 Ha $Å^{-1}$ and 0.005 Å, respectively.

Molecular dynamics (MD) simulations

All MD simulations were carried out in Large-scale Atomic/Molecular Massively Parallel Simulator (LAMMPS).[S12] The visualisation was conducted with 3D visualisation Open Visualisation Tool (OVITO).[S13] Based upon the thermodynamically stable structure of TpPa-$SO_3Zn_{0.5}$ obtained from DFT calculation, a 4 × 4 × 54 supercell was constructed. The carbon atoms of the framework were assumed to be dynamically rigid. H_2O was saturated in the pores of TpPa-$SO_3Zn_{0.5}$ for similarity with the experimental conditions. An LE system with the same magnitude was constructed by a fixed density of 1.31 g cc^{-1} for 2 M $ZnSO_4$ in H_2O. Both systems were equilibrated with *NVT* ensemble at 298 K for 2 ns. After then, an external electric field of 1.0 V $Å^{-1}$ in the $-z$-axis direction was applied to the systems for 3 ns. The Zn^{2+} number density profiles, velocity distributions and fraction of Zn–O coordination numbers were obtained by analysis of average trajectories during the last 1 ns of this stage.

The Nose–Hoover thermostat was used to control temperature.[S14] The Assisted Model Building with Energy Refinement (AMBER) force field[S15] was used for both TpPa-$SO_3Zn_{0.5}$ and LE systems. The optimised AMBER force field for SO_4^{2-},[S16] the optimised non-bonded interaction for Zn^{2+},[S17] the general AMBER force field (GAFF)[S18] for the other atoms were used for this analysis. The Mulliken charge[S19] obtained from the DFT calculation was assigned as a partial atomic charge for all systems.

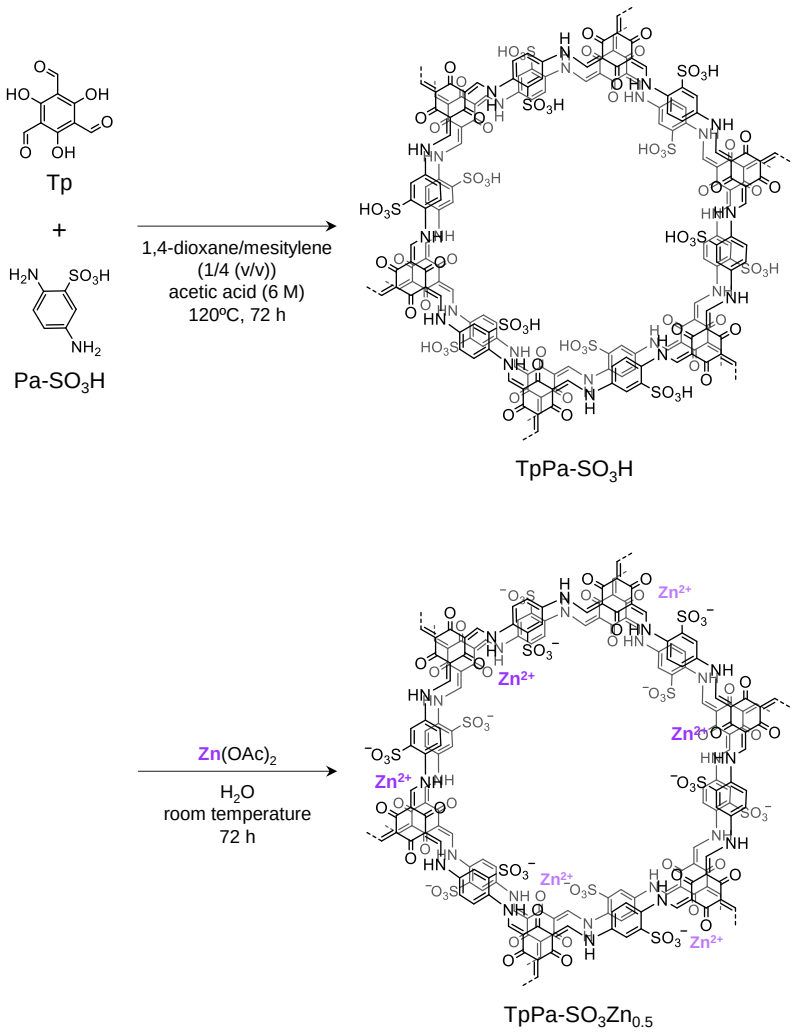

Scheme S1 Synthesis of TpPa-$SO_3Zn_{0.5}$.

Tables

Table S1 CHN analysis and ICP-OES (for Zn) results for TpPa-$SO_3Zn_{0.5}$

	C	H	N	Zn
Calcd. (wt%) for $C_{72}H_{42}N_{12}O_{30}S_6Zn_3$	44.49	2.18	8.65	10.09
Found (wt%)	44.32	2.62	8.79	9.82

Table S2 Unit cell parameters of TpPa-$SO_3Zn_{0.5}$

	TpPa-$SO_3Zn_{0.5}$
Formula	$C_{72}H_{42}N_{12}O_{30}S_6Zn_3$
Symmetry	Triclinic
Space group	*P*1
a (Å)	22.8345
b (Å)	22.9434
c (Å)	6.8744
α (º)	89.8514
β (º)	89.7964
γ (º)	120.5433

Table S3 $t_{Zn^{2+}}$ values of TpPa-$SO_3Zn_{0.5}$ and previously reported Zn^{2+} conducting polyanions

Anionic host	Guest	$t_{Zn^{2+}}$	Ref.
Zinc sulfonated COF (TpPa-$SO_3Zn_{0.5}$)	H_2O	0.91	This study
Zn^{2+}-paired anionic MOF (ZnMOF-808)	H_2O	0.93	S20
Zinc sulfonated poly(ether ether ketone) (Zn-SPEEK)	H_2O	0.89	S21
Sulfonated perfluoro polyolefin (3M-Nafion)	3 M $ZnSO_4$ in H_2O	0.52	S22
Zinc sulfonated perfluoro polyolefin (ZPSAM)	H_2O	0.2	S23

Table S4 Details on model systems constructed for MD simulations

		TpPa-$SO_3Zn_{0.5}$	LE (2 M $ZnSO_4$ in H_2O)
Number of species	Zn^{2+}	2592	3216
	TpPa-SO_3^-	1 (139968 atoms)	–
	SO_4^{2-}	–	3216
	H_2O	46656	89208
Total number of atoms		282528	286920
Cell parameters	*a* (Å)	91.34	
	b (Å)	91.77	
	c (Å)	371.22	
	α (°)	90	
	β (°)	90	
	γ (°)	120	

Table S5 Characteristics of electrochemical cells containing TpPa-$SO_3Zn_{0.5}$ compared with those containing previously reported single Zn^{2+} conductors

Single Zn^{2+} conductor	Cycling time of the Zn‖Zn cell, h (current density, mA cm^{-2} ; capacity, mAh cm^{-2})	Battery application (operating voltage, V)	Cycle number (current density, A g^{-1})	Ref.
Zinc sulfonated COF (TpPa-$SO_3Zn_{0.5}$)	500 (0.1; 0.1)	Zn‖MnO_2 (*ca.* 1.4)	800 (0.6)	This study
Zn^{2+}-paired anionic MOF (ZnMOF-808)	360 (0.1; 0.05)	Zn‖VS_2 (*ca.* 0.7)	250 (0.2)	S20
Zinc sulfonated poly(ether ether ketone) (Zn-SPEEK)	50 (1; 0.5)	–	–	S21
Sulfonated polyacrylonitrile (PAN-S)	350 (0.5; 0.25)	–	–	S24

Figs.

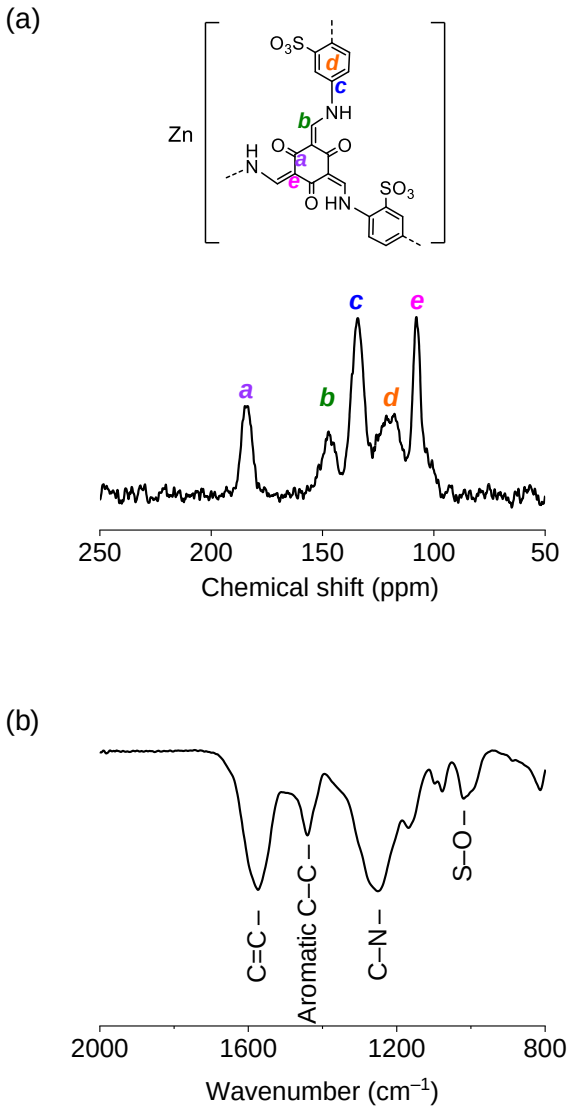

Fig. S1 (a) CP-MAS ^{13}C NMR and (b) FT-IR spectra of TpPa-$SO_3Zn_{0.5}$.

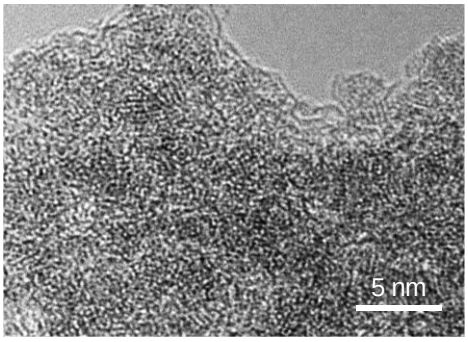

Fig. S2 TEM image of TpPa-$SO_3Zn_{0.5}$.

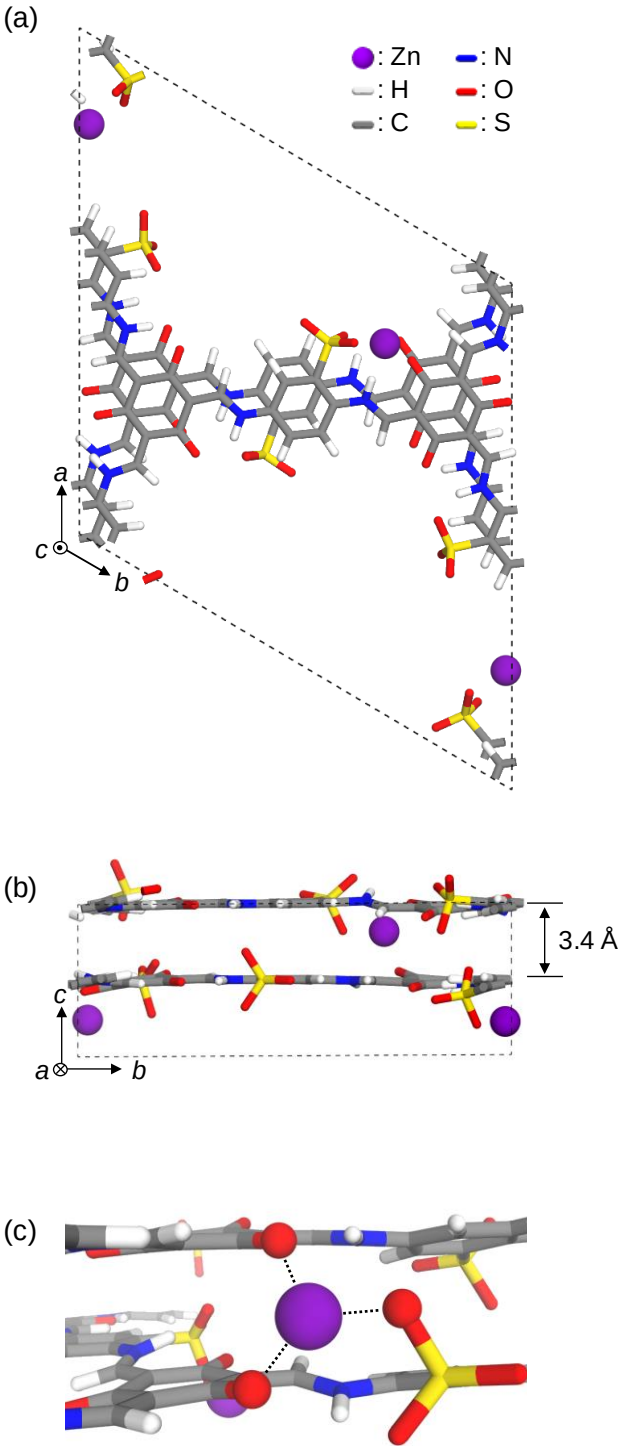

Fig. S3 Theoretical unit cell structure of TpPa-$SO_3Zn_{0.5}$ displayed along (a) *c*- and (b) *a*-axes. (c) Optimal geometry of Zn^{2+}.

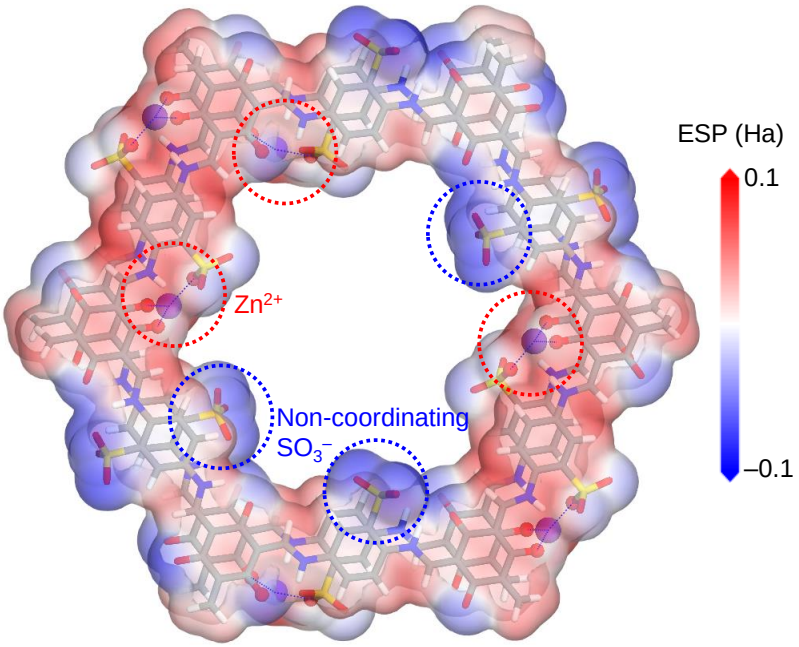

Fig. S4 Electrostatic potential (ESP) for TpPa-$SO_3Zn_{0.5}$ mapped on the electron density surface.

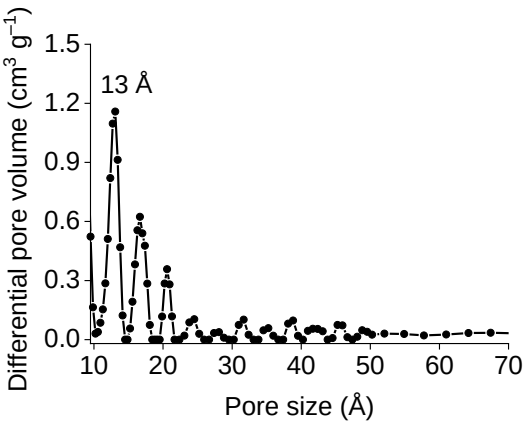

Fig. S5 Pore size distribution of TpPa-$SO_3Zn_{0.5}$.

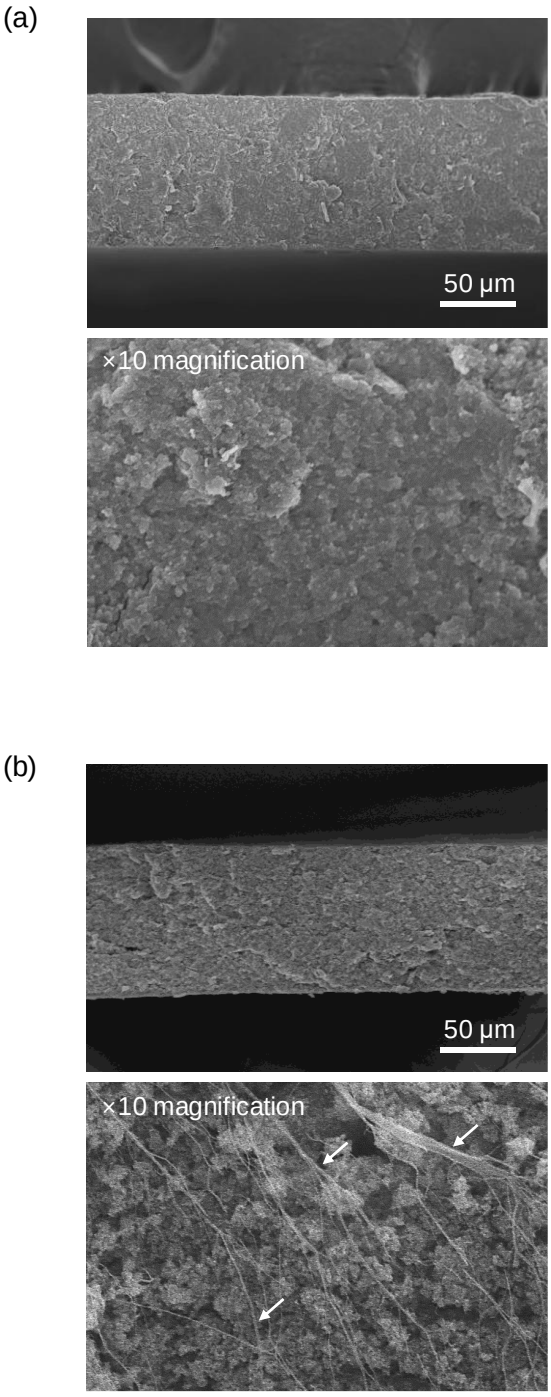

Fig. S6 Cross-sectional SEM images of (a) a TpPa-$SO_3Zn_{0.5}$ pellet and (b) a TpPa-$SO_3Zn_{0.5}$–PTFE composite membrane (arrows: PTFE fibres).

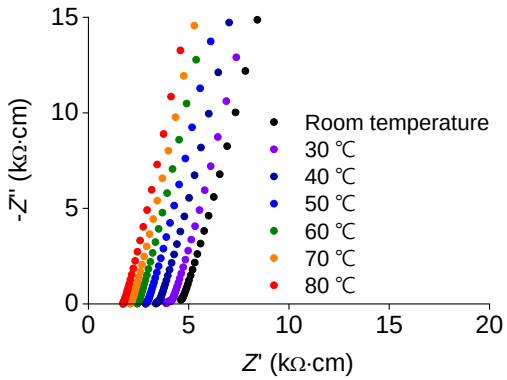

Fig. S7 EIS profiles of the hydrated TpPa-$SO_3Zn_{0.5}$ measured at varied temperatures.

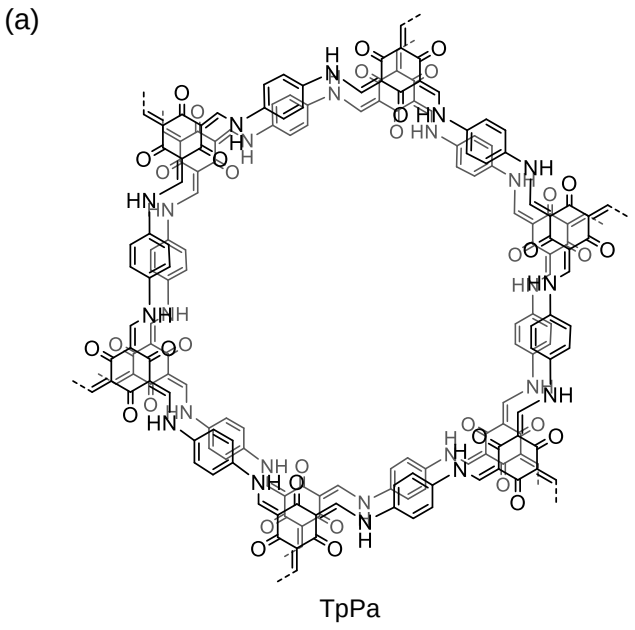

Fig. S8 (a) Chemical structure, (b) XRD patterns and (c) N_2 gas isotherms of TpPa.

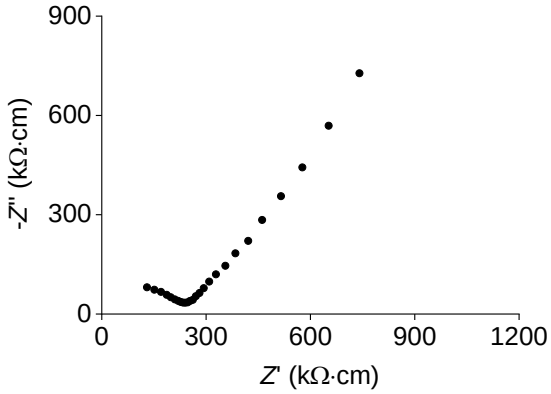

Fig. S9 EIS profile of the hydrated TpPa measured at room temperature.

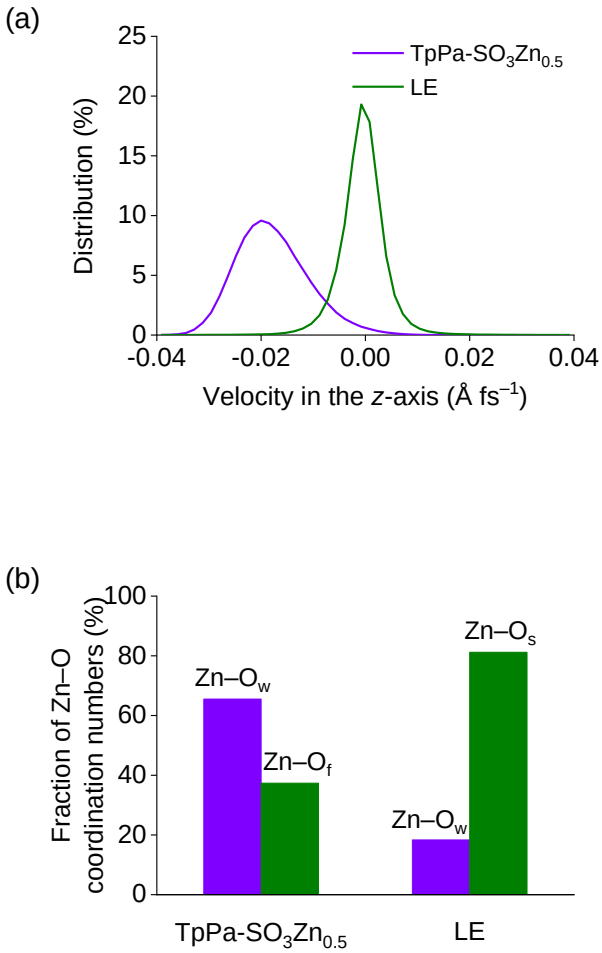

Fig. S10 (a) Velocity distribution of Zn^{2+} in TpPa-$SO_3Zn_{0.5}$ and LE (2 M $ZnSO_4$ in H_2O) in the *z*-axis. (b) Fraction of Zn–O coordination numbers in TpPa-$SO_3Zn_{0.5}$ and LE. O_w belongs to H_2O, O_f belongs to TpPa-SO_3^- and O_s belongs to SO_4^{2-}.

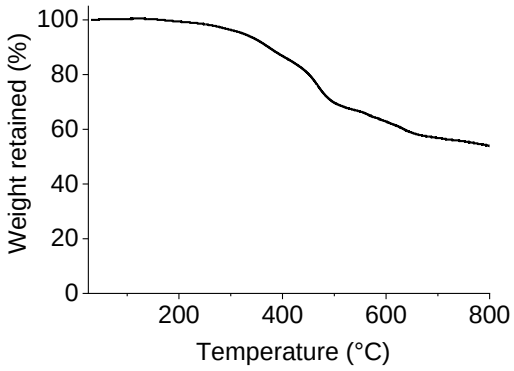

Fig. S11 TGA curve of TpPa-$SO_3Zn_{0.5}$.

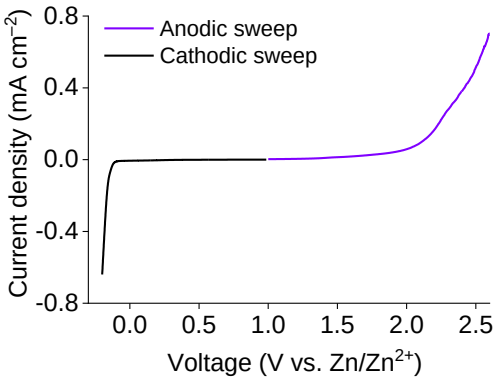

Fig. S12 LSV profile of TpPa-$SO_3Zn_{0.5}$.

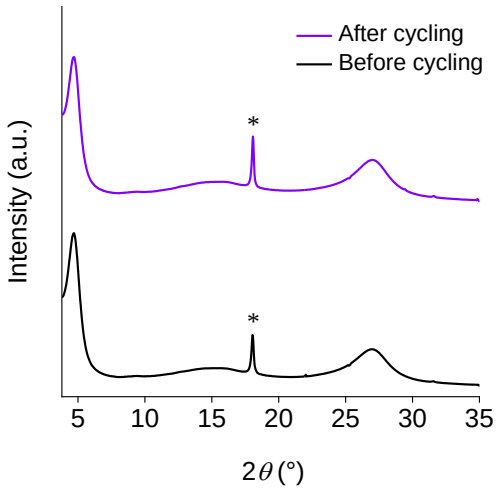

Fig. S13 XRD patterns of TpPa-$SO_3Zn_{0.5}$ (as a PTFE composite membrane) before and after the Zn plating/stripping test. *PTFE.

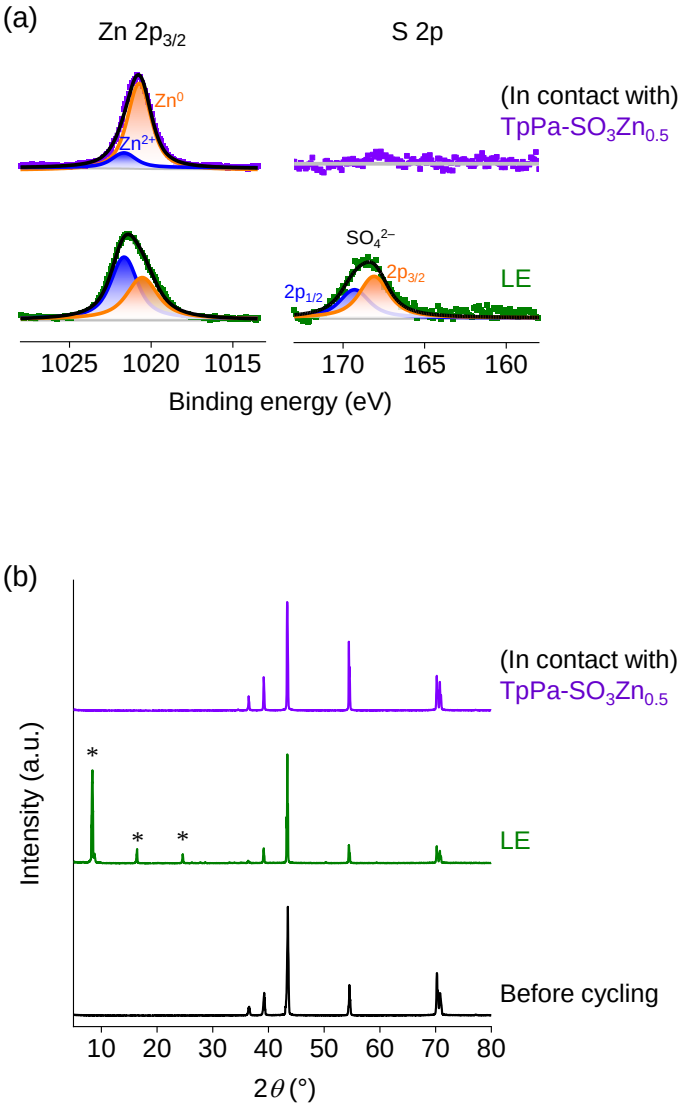

Fig. S14 (a) XPS spectra (Zn $2p_{3/2}$ and S 2p) of Zn metal electrodes after Zn plating/stripping tests in contact with TpPa-$SO_3Zn_{0.5}$ (top) or LE (2 M $ZnSO_4$ in H_2O; bottom). (b) XRD patterns of Zn metal electrodes before (black) and after Zn plating/stripping tests in contact with TpPa-$SO_3Zn_{0.5}$ (purple) or LE (green). *$Zn_4SO_4(OH)_6 \cdot 5H_2O$ (PDF 39-0688).

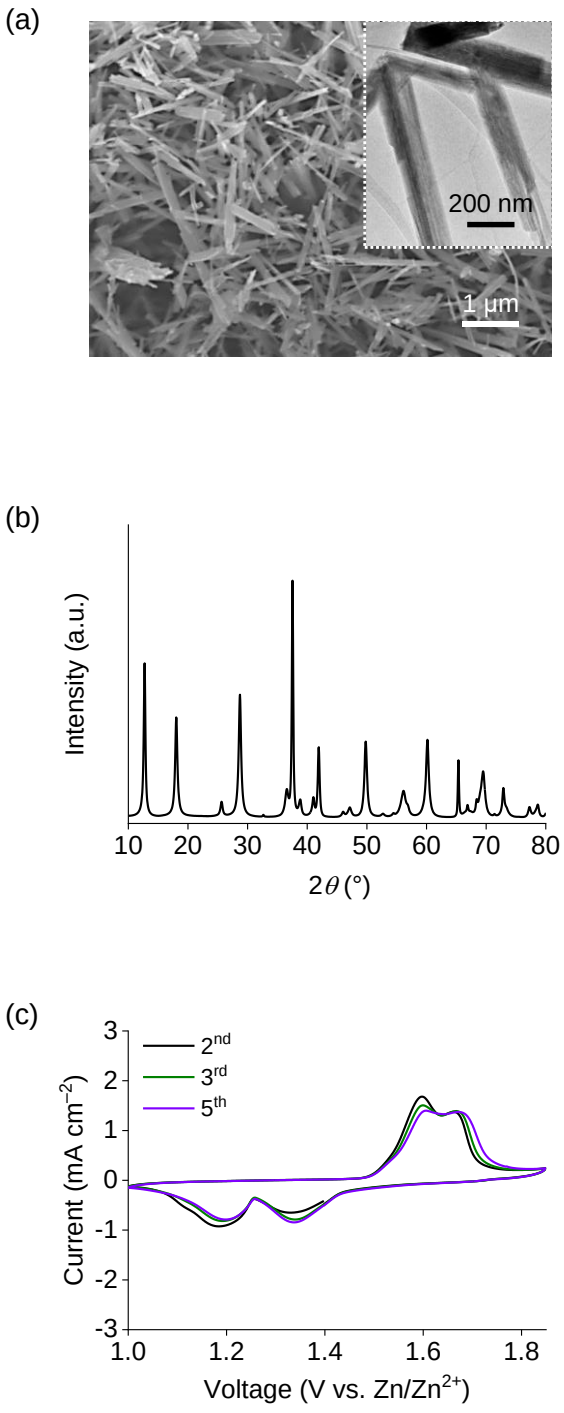

Fig. S15 (a) SEM and TEM (the inset) images, (b) XRD pattern (PDF 44-0141) and (c) cyclic voltammograms of α-MnO_2.

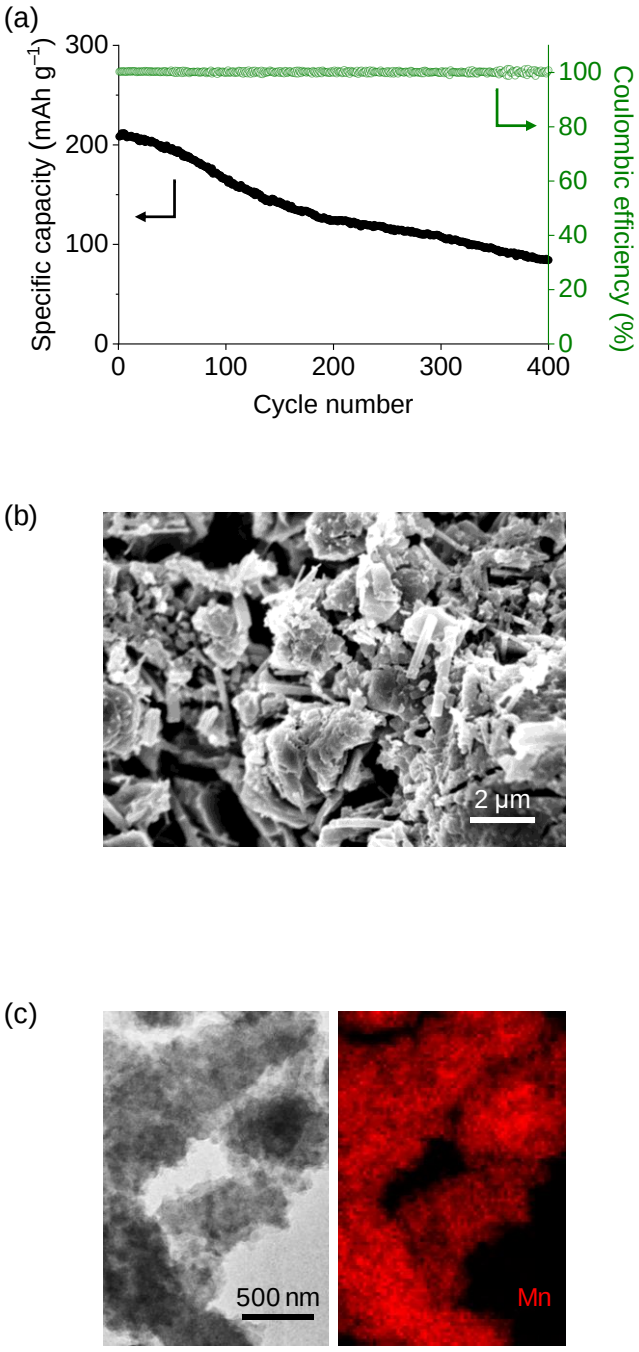

Fig. S16 (a) Cycling performance of a Zn|LE|MnO_2 cell (LE = 2 M $ZnSO_4$ + 0.2 M $MnSO_4$ in H_2O). (b) SEM image of the Zn metal anode after the 400th cycle. (c) TEM (left) and EDS mapping (for Mn; right) images of the MnO_2 cathode after the 400th cycle.

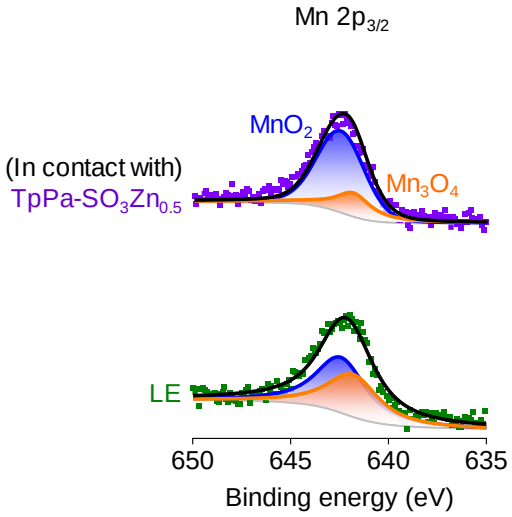

Fig. S17 XPS spectra (Mn $2p_{3/2}$) of MnO_2 cathodes cycled in contact with TpPa-$SO_3Zn_{0.5}$ (top) or LE (2 M $ZnSO_4$ + 0.2 M $MnSO_4$ in H_2O; bottom).

References

S1 J. H. Chong, M. Sauer, B. O. Patrick and M. J. MacLachlan, *Org. Lett.*, 2003, **5**, 3823–3826.

S2 K. Jeong, S. Park, G. Y. Jung, S. H. Kim, Y.-H. Lee, S. K. Kwak and S.-Y. Lee, *J. Am. Chem. Soc.*, 2019, **141**, 5880–5885.

S3 S. Chandra, T. Kundu, K. Dey, M. Addicoat, T. Heine and R. Banerjee, *Chem. Mater.*, 2016, **28**, 1489–1494.

S4 S. Kandambeth, A. Mallick, B. Lukose, M. V. Mane, T. Heine and R. Banerjee, *J. Am. Chem. Soc.*, 2012, **134**, 19524–19527.

S5 H. Pan, Y. Shao, P. Yan, Y. Cheng, K. S. Han, Z. Nie, C. Wang, J. Yang, X. Li, P. Bhattacharya, K. T. Mueller and J. Liu, *Nat. Energy*, 2016, **1**, 16039.

S6 J. Evans, C. A. Vincent and P. G. Bruce, *Polymer*, 1987, **28**, 2324–2328.

S7 B. Delley, *J. Chem. Phys.*, 1990, **92**, 508–517.

S8 B. Delley, *J. Chem. Phys.*, 2000, **113**, 7756–7764.

S9 J. P. Perdew, K. Bruke and M. Ernzerhof, *Phys. Rev. Lett.*, 1996, **77**, 3856–3868.

S10 A. Tkatchenko and M. Scheffler, *Phys. Rev. Lett.*, 2009, **102**, 073005.

S11 H. J. Monkhorst and J. D. Pack, *Phys. Rev. B*, 1976, **13**, 5188–5192.

S12 S. Plimpton, *J. Comp. Phys*., 1995, **117**, 1–19.

S13 A. Stukowski, *Modelling Simul. Mater. Sci. Eng.*, 2010, **18**, 015012.

S14 W. G. Hoover, *Phys. Rev. A*, 1985, **31**, 1695–1697.

S15 W. D. Cornell, P. Cieplak, C. I. Bayly, I. R. Gould, K. M. Merz Jr., D. M. Ferguson, D. C. Spellmeyer, T. Fox, J. W. Caldwell and P. A. Kollman, *J. Am. Chem. Soc.*, 1995, **117**, 5179–5197.

S16 S. Kashefolgheta and A. V. Verde, *Phys. Chem. Chem. Phys.*, 2017, **19**, 20593–20607.

S17 P. Li, B. P. Roberts, D. K. Chakravorty and K. M. Merz Jr., *J. Chem. Theory Comput.,* 2013, **9**, 2733–2748.

S18 J. Wang, R. M. Wolf, J. W. Caldwell, P. A. Kollman and D. A. Case, *J. Comput. Chem.*, 2004, **25**, 1157–1174.

S19 R. S. Mulliken, *J. Chem. Phys.*, 1955, **23**, 1833–1840.

S20 Z. Wang, J. Hu, L. Han, Z. Wang, H. Wang, Q. Zhao, J. Liu and F. Pan, *Nano Energy*, 2019, **56**, 92–99.

S21 C. Hänsel and D. Kundu, *ACS Omega*, 2019, **4**, 2684–2692.

S22 M. Ghosh, V. Vijayakumar and S. Kurungot, *Energy Technol.*, 2019, **7**, 1900442.

S23 Y. Cui, Q. Zhao, X. Wu, Z. Wang, R. Qin, Y. Wang, M. Liu, Y. Song, G. Qian, Z. Song, L. Yang and F. Pan, *Energy Storage Mater.*, 2020, **27**, 1–8.

S24 B.-S. Lee, S. Cui, X. Xing, H. Liu, X. Yue, V. Petrova, H.-D. Lim, R. Chen and P. Liu, *ACS Appl. Mater. Interfaces*, 2018, **10**, 38928–38935.